Original article

Biodegradation effects of three *Aspergillus* species on iron-based oxides (Hematite – Goethite) in paint layer in oil paintings

Abatable Thanaa [a], Mari Sumayli [b], A. El-Shabasy [b],*

[a] *The Faculty of Archaeology, Aswan University, Egypt*
[b] *Department of Biology, College of Science, Jazan University, P.O. Box. 114, Jazan 45142, Kingdom of Saudi Arabia*

ARTICLE INFO

ABSTRACT

The inorganic colour layer based on iron oxide is affected by microorganisms (fungi) and leads to its deterioration due to feeding on the mineral elements through the chemical composition of the colour in the presence of a suitable environment (medium). Damage occurs as a result of heavy metal elements being removed from the colour, leading to a defect in the chemical composition and the fading of the colours. The current study showed the effect of the different types of the most common fungi on oil paintings (*Aspergillus flavius, Aspergillus fumigatus* and *Aspergillus niger*) after cultivating the different types of fungi and obtaining pure colonies for each fungus separately and conducting a fungal infection on experimental samples with preparing the old techniques, coloured with hematite red and goethite yellow. Each colour is mixed with different proportions of linseed oil (1, 2, 3). They were aged artificially and incubated at a temperature of 26^{2+} degrees and examined periodically until the fungi appeared on the surface in the form of colour spots ranging from very dark (severe infestation) to light (low infestation). The change in chemical composition was measured by Raman and EDX analyses of the samples before and after infection. Fungi showed the appearance of spoilage products from metal sulfides and metal carboxylates. The iron oxide ion decreased in both the red and the yellow colours, leading to a change after the fungal infection. Examination of the morphological surface using SEM, USB and measurement of colour change showed the change in the red colour more than the yellow and scattering of green and black colour dots on the surface of the sample. Correlation and Simple Linear Regression were applied for each colour before and after besides both colours together. It was found that these colours appeared around some of the fungal colonies as a result of the activities. Fungal species of some strains reduced Fe^{+3} to Fe^{+2}. This provides new insights into the role of microorganisms in the deterioration of painted surfaces.

1. Introduction

Biological degradation plays a major role in the deterioration of works of art and antiquities composed of organic and inorganic materials which consequently cause aesthetic and structural damage (Ranalli et al., 2009). Since the organic chemical metabolism and/or microbial chemical/photochemical metabolism depends on the chemical nature of the materials, A full understanding of the microbial diversity and materials in a work of art may provide useful information for restoration and conservation. Many studies have been done on the microbial colonization of damaged stone monuments fresco (Videla et al., 2000), but few studies have described the microbial communities living on easel paintings. Wooden, applied to canvas or wood panels and this type of Works of art contains nutrients suitable for the growth of

microorganisms, such as organic materials (pigment, medium, varnish) (Pellerito et al., 2016) and inorganic materials (pigment) (Gargano et al., 2020). Microbial growth occurs in the support layer (canvas, wood, paper, etc.), the materials used to in the paint layers (pigment, oil), or the compounds used to adhere to the film (animal glue) in environmental conditions suitable for their growth, such as high relative humidity, which may accelerate the growth of microorganisms (Matteini & Mazzeo, 2009).

Earth oxide colours on the surface of oil paintings are attacked by fungi, and these microorganisms absorb minerals that may be present in inorganic colours such as hematite and goethite to feed on them and taking their elements that make up the colours for the purpose of completing metabolic processes, causing damage to paints layer (Salvador et al., 2017), Heavy metals have an effect on growth,

development, and metabolic processes that fungi need in order to complete their lives. These organisms exploit the heavy metal elements that are present within the chemical composition of colour, and derive these elements and feed on them.This is done through a process known as the absorption process, and it occurs as a result of the chemical and physical interactions that occur between metal ions and cellular compounds of biological types, which work to partially decompose the coloured materials, which leads to the loss of their cohesion and the fading of these colourings, and also, from a physical standpoint, the occurrence of deformation due to the resulting stains of these fungi. These organisms cause damage in two ways. The first is directly when the materials used in the manufacture of the painting are used for the growth of microorganisms as a suitable environment for growth or the absorption of elements that are present in colours with metallic oxides, such as the iron element in coloured materials such as red and yellow ochre, given that iron is necessary for the growth and spread of the vast majority of organisms. Microorganisms which reduce the ferric ion, Fe^{+3}, to the ferrous ion, Fe^{+2} due to the ease of absorption of the ferrous ion from the ferric ion to carry out the vital processes of living organisms (Kosman, 2003).

The second method is indirect one that is the production of enzymes and acids resulting from organisms performing these vital processes, which interact with inorganic colours, causing severe damage to the colours. Among the factors that create ideal conditions for the growth of such organisms on the surface of the antiquity are temperature, relative humidity, light and pH level. It also works to change the colour or turn it into another colour due to a loss in the proportions of the colour elements itself. Fungi also work by using reductive enzymes or low-molecular-weight iron-reducing agents to reduce ferric ions to ferrous ions. Fungal growth on colours also works to hide appearances, distorts the general appearance of the effect, and causes deterioration of the layers of the painting, as of hypha penetrates the layers of the painting, secretes organic and inorganic acids, and produces extracellular enzymes, which lead to the deterioration of the colours, their separation, cracking, and loss from the pictorial layers, as well as colour changes and its appearance (Poyatos et al., 2018; Cañveras et al., 2001).

The microscope is used to obtain detailed information about the state of deterioration, the microbiological surface of the painting (Grbić et al., 2016). Nowadays, many biochemical and petrographic tests are used to study biochemical deterioration, which helps in assessing potential risks to cultural heritage pieces (Savković et al., 2019). Raman spectroscopy analysis was used to identify oxalates, which often appear in the form of a layer on the surface of paintings besides damage products from inorganic materials that lead to colour deterioration. SEM-EDX techniques study the decomposition of inorganic colours as well as how the decomposition products are transported and interact with other layers of paint (Frost & Weier, 2003).

The current study showed the effect of the different types of the most common fungi (*Aspergillus flavius, Aspergillus fumigatus* and *Aspergillus niger*) on oil paintings with hematite red and goethite yellow by measuring the change in chemical composition by Raman and EDX analyses besides morphological surface by using SEM and USB to evaluate the degree of deterioration occurred by fungi.

2. Materials and methods

2.1. Sample preparation simulated painting models

Samples had been prepared according to the traditional technical methods of ancient oil painting (Cucci et al., 2016; Onofri, 2009, Berg et al., 2000, De Viguerie et al., 2009, Bruyn et al., 2012, Armstrong-Totten, 2014). The swatch had been prepared linen fabric plain weave 1/1, undyed, linear density 16, 194 g/m2 coat applied from the glue on the canvas, the ground was spread on the canvas after the glue consisting of animal glue and calcium carbonate, then kept at room temperature for 72 h at 25 ± 2 °C until dry. After that, the white ground layer was covered with a layer of colours of hematite red and goethite yellow. Each colour was applied individually to the surface mixed with a different ratio of linseed oil (1:2:3) in three samples for each colour, and the total number of samples were 6 samples. All pigments were coarser; the particle size was less than 45 μm. The binder used was linseed oil from Royal Talens Headquarters co. Sophialaan 46, 7311 PD Apeldoorn, Netherlands. The mixed colour was applied to a canvas an area 1 cm x 1 cm by brush of then left for 6 months to dry. The samples were subjected to accelerated artificial thermal aging in a laboratory oven at a temperature of 105 ± 1 °C in the absence of light for 357 h. The results were obtained in the natural aging of the painting on canvas at 25 °C for 160 years (Seves et al., 2000) as (Fig. 1).

2.2. Growing fungi in the media

The Petri dishes and glass tools were sterilized in the autoclave at a temperature of 121 °C for 20 min. The sterilized Petri dishes were filled with the prepared medium of 200 g of Potato Dextrose (PD) medium, and streptomycin was added as an antibiotic to prevent the growth of bacteria so that we could obtain pure fungal growth, then the environment was poured into petri dishes and left to cool, thus the isolation environment became ready for fungal growth. The most common fungi in oil paintings were chosen; *Aspergillus fumigatus*, *Aspergillus niger* and *Aspergillus flavus*. The fungi were grown and purified, and pure colonies were obtained for each fungus separately (Poyatos et al., 2018; Carvalho et al., 2019) (Plate 1, Table 1).

2.3. Fungal infection on colour samples

The microbial solution was prepared and the three fungi were inoculated upon the red and yellow colour samples mixed with linseed oil in at ratio of (1 oil: 1 colour / 2 oil: 1 colour / 3 oil: 1 colour) in petri dishes, thus producing 6 dishes for the two colours (red − yellow). They were incubated at a temperature of 27 °C for a period of not less than a month and a half, with the humidity of the dishes increasing weekly. Incubation was done until the fungi grew completely to cover the colours, then it was incubated in the dark at a temperature of 26 ± 2 °C for two weeks until the fungi appeared on its surface. Conducting the artificial infection processed with a fungal suspension on colours while observing the fungal growth daily and checking the humidity besides temperature levels during the period from 10 days to 21 days until the fungal growth appeared on the surface in the form of colour spots that vary from dark (severe infection) to low colour incidence (less infection) **(Koschan & Abidi, 2008)**.

2.4. Morphological characterization

2.4.1. Colourimetric examination
The colour content of the samples was measured after the rate of change ΔE* was equal to or less than 3. The colour change was not perceptible to the human eye and values higher than 3.5 were considered clearly visible. The colourimetric measurements of the samples before and after the fungal infection were done using a portable colourimeter type (PCE-CSM7 S/ N 330,242 made in UK) (Monaco et al., 2011).

2.4.2. USB and SEM examination
USB digital microscope and the scanning electron microscope (SEM) showed the spread of fungal hyphae on the surface and the resulting damage. They were 1080P Full HD WiFi Digital microscope Olympuse DP 731 model and JEOL JSM 5400 LV EDX Link ISIS − Oxford detector "high vacuum" model.for both USB and SEM respectively.
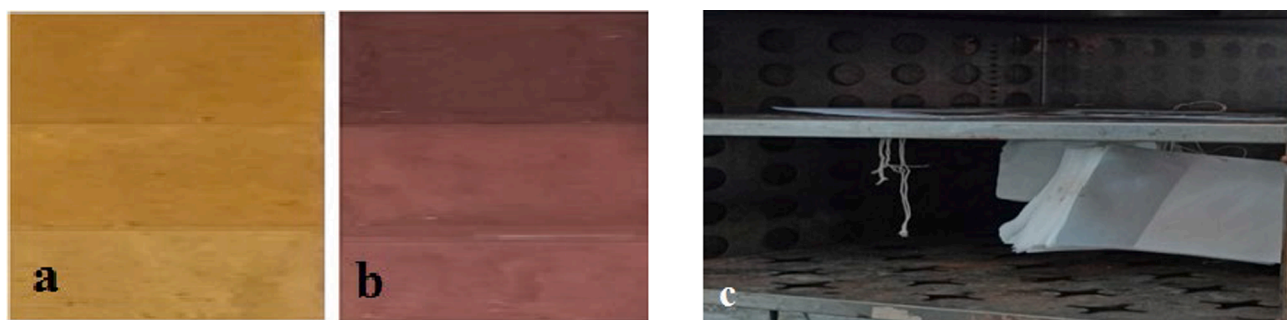
Fig. 1. Samples prepared by traditional technical methods of ancient oil painting, a. goethite yellow, b. hematite red, c. thermal aging of painting.
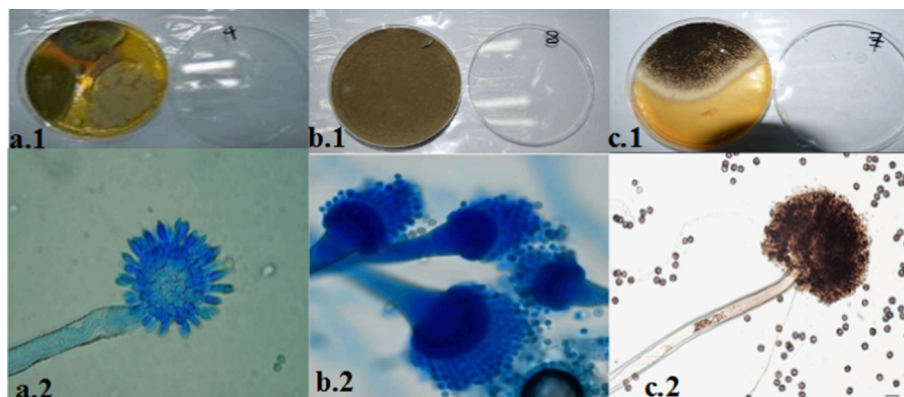

Plate 1. Fungal growth on (PDA) plates and their appearance under light microscope, a. *Aspergillus flavus*, b. *Aspergillus fumigatus*, c. *Aspergillus niger*.

Table 1
Morphological features among studied *Aspergillus* sp.

	Aspergillus flavus	*Aspergillus fumigatus*	*Aspergillus niger*
Conidia	globose, thin walled, slightly roughed	globose to prolate	finely wrinkled-wrinkled, globular-ellipsoidal
Conidiophores	colourless, thick walled, roughed	colourless, thick walled, roughed	A dark brown colour, long, thin walled, smooth
Diameter of conidia	2.5–4.5 µm	1.5–2.5 µm	3–5 µm
Diameter of conidiophores	800–1200 µm	150–300 µm	100–3000 µm
Hyphae	uniseriate or biseriate	uniseriate	biseriate
Vesicles	globose to sub-globose	ovate to flask shape	globule
Vesicles diameter	25–30 mm	15–25 mm	20–73 mm
Phialides	ampuliform	ampuliform	ampuliform
Sterigmata	biseriates	uniseriates	biseriate

2.5. Chemical characterization

2.5.1. EDX microanalysis

Energy Dispersive X-ray (EDX) microanalysis was done to determine the percentages of mineral oxides before and after fungal infection. Model JEOL JSM 5400 LV EDX Link ISIS – Oxford detector "high vacuum" was used.

2.5.2. Raman analysis

Samples were analysed and examined by using Raman microscope (SENTREEA π) with 20X magnification and 785 nm laser with a power of 10 microwatts in a time of 10 s. The colours were determined by comparing the experimental spectrum with the standard spectrum.

Some compounds were extracted for spoilage products while monitoring the colour changes that were not apparent as a result of crowding on the chart through millimetre calque paper because there were numbers included in the crowded curve.

2.6. Statistical analysis

Correlation analysis described the extent of co-variation among studied data. The Simple Linear Regression (SLR) equation represented the correlated data in the form of scattered plot graphs (Abada et al., 2024).

3. Results

3.1. Colourimetric measurements

Measurement of the colour changed before and after infection with the fungus was carried out on samples of red and yellow colours mixed with different proportions of linseed oil. It resulted that the red sample [1 colour: 1 oil] had a change after the fungal infection, and a decrease in all the values of [a*, b*, L*] appeared, so the value of L* decreased from (87.09 to 43.25), [a*] decreased from (29.91 to 12.05), and [b*] decreased from (96.16 to 45.98), a red colour sample [1 colour: 2 Oil] changed after the fungal infection all the values of [a* L*, b*] decreased, L* decreased from L* decreased from(87.19 to 76.23), (a*) from (15.45 to − 2.09), and b* Changed from (51.17 to 26.75). The red colour sample [1 colour: 3 oil] changed after the fungal infection that all the values of [a*, b*, L*] decreased, L* from(65.25 to 17.09), a* changed from 23.13 to 5.27, and b* changed from(61.14 to 19.61).

The yellow colour sample [1 colour: 1 oil] changed after the fungal infection that all the values of [a*,*L, b*] decreased L* decreased from (87.09 to 43.25), a* from (29.91 to 12.05), and b * from (69.16 to 45.98), and the yellow colour sample [1 colour: 2 oil] had a change after

the fungal infection, so all the values of [L*, b*, a*] decreased, *L decreased from (88.19 to 77.23), a* from (14.45 to −1.09), and b* changed from (50.17 to 25.75). Colour sample [1 colour: 3 oil] change after the fungal infection, and all the values of [L*, b*, a*] decreased, L* decreased from (65.25 to 17.09), and a* decreased from (32.31 to 5.27) and b* from (61.41 to 19.61). The rate of colour change was measured according to (Bacci et al., 1991):

$$\Delta E^*_{ab} = \sqrt{\left(L^*_2 - L^*_1\right)^2 + \left(a^*_2 - a^*_1\right)^2 + \left(b^*_2 - b^*_1\right)^2}$$

The rate of change of yellow colour sample (1 colour: 3 oil) exhibited the highest value (ΔE = 69.2), followed by red in the same ratio (1 colour: 3 oil) (ΔE = 58.1) (Tables 2 and 3) (Plate 2).

3.2. Examination and analysis by SEM-EDX

Analysis of the red colour sample mixed with linseed (1 oil:1 colour) confirmed that the presence of sodium oxide by 6.46 %, aluminum oxide by of 5.04, calcium oxide by of 49.77, and iron oxide by 53.12 while samples infected with fungi was decreased a difference in the percentages of both sodium oxide were by 2.04. %, aluminum oxide by 1.06 %, calcium oxide by 43.54 %, the of iron oxide decreased by 8.67 % in appearance of sulphur dioxide by 10.82 % and phosphorus oxide by 12.46 % (Fig. 2 **a, b**) The SEM of the same sample before aging showed the homogeneity of the grains and after aging. Heterogeneity changed the morphological surface and displacement of some elements on the surface (Lepot et al., 2006). Cracks, colour, penetration of cracks by fungi and formation of paint blisters were also observed (Plate 3 **a, b**).

The change in the morphological surface in some red areas was explained as a result of environmental conditions suitable for fungal growth. It resulted in the decomposition of colour and the release of iron, so the percentage of Fe content decreased which indicated that Fe formed a distinct mineral of the (iron oxides) phase. EDX analysis of the red colour sample mixed with linseed oil by (2 oil: 1 colour) confirmed the presence of sodium oxide at a rate of 6.20 %, aluminium oxide by 4.55 %, calcium oxide by 29.53 %, and iron oxide by 36.24 %. As for the samples infected with fungi, it was noted that the rates of oxides differed, as the rates of both sodium oxide decreased by 0.03 %, calcium oxide by 28.29 %, the percentage of iron oxide decreased by 5.07 %, aluminium oxide by 1.12 %, the appearance of sulphur dioxide by 4.60 %, and phosphorus oxide by 2.21 %, (Fig. 2 **c, d**). Before aging, the SEM showed uniformity of grains while after aging, lack of uniformity and cracking, the formation of paint blisters and an increase in dark spots resulted from the secretion of fungi (Plate 3 **c, d**). EDX analysis of the red colour sample mixed with linseed oil at a ratio of (3 oil: 1 colour) The presence of sodium oxide by 9.50 %, aluminium oxide by 14.72 %, calcium oxide by 37.98 %, and iron oxide by 51.44 %. As for the samples infected with fungi, it was decreased. Sodium oxide by 2.51 %, calcium oxide by 15.15 %, iron oxide is 2.70 % aluminium oxide by 1.08 %, sulphur dioxide by 13.59 % and phosphorus oxide by 12.45 % (Fig. 2 **e, f**). SEM of the same sample before aging showed the homogeneity of the grains and the regularity of the surface, and after aging, the surface was uneven, cracked with the penetration of fungal hyphae into the colour layer (Plate 3 **e, f**).

EDX analysis of the yellow colour sample mixed with linseed oil by (1

oil: 1 colour) **Figure (3 a, b)**, confirmed that the presence of sodium oxide by 17.98 %, aluminum oxide by 11.96 %, sulphur dioxide by 8.81 %, calcium oxide by 49.54 %., and iron oxide by 45.89 %. As for the samples infected with fungi, the ratios of oxides decreased.

Sodium oxide was to 5.96 %, aluminum oxide by 1.30 %, iron oxide by 2.03 %, sulphur dioxide by 19.74 %, calcium oxide by 4.41 %, and the appearance of phosphorus oxide by 8.37 %, The SEM showed the homogeneity of the granules before infected but after infected with fungi, heterogeneity and disintegration of the granules and their weakness on the surface were occurred (Montagner et al., 2013). The medium and colours lost the strength of cohesion between the atoms which resulted in the particles appearing clearly on the surface where suffered from concavity and a change in the mechanical properties of the paint thus the morphological features of the crystals seen on the surface (Plate 4 **a, b**). EDX analysis of the yellow colour sample mixed with linseed oil in a ratio (2 oil: 1 colour) (Fig. 3 **c, d**) showed the presence of sodium oxide by 12.30 %, aluminum oxide by 6.80 %, sulfur dioxide by 10.26 % and calcium oxide by 48.73 % and iron oxide by 26.89 %. The samples infected with fungi exhibited a difference in the percentages of oxides. The percentage of aluminum oxide decreased by 5.24 %, calcium oxide by 2.51 %, the percentage of iron oxide decreased by 8.49, sodium oxide by 3.72 %, the percentage of sulfur dioxide increased by 12.96 %, and the appearance of phosphorus oxide by 12.86 %. The SEM of the colour sample mixed with a ratio of (2 oil: 1 colour) showed before infected the flatness of the surface and the homogeneity of the grains. After being infected, exposure to fungal damage caused the fungus to penetrate the colour layer and spread, the disintegration of the grains, the displacement of metal atoms on the surface and the formation of cracks that developed as a result of the increase in fungal hyphae, which caused the formation of pimples and pits (Plate 4 **c, d**).

EDX analysis of the yellow colour sample mixed with linseed oil in a ratio (3 oil: 1 colour), (Fig. 3 **e, f**), showed the presence of sodium oxide by 20.19 %, aluminum oxide by 14.06 %, sulfur dioxide by 5.34 %, and calcium oxide by 28.53 %, iron oxide by 40.58 %. It was reported that the samples which infected with fungi, had a difference in the percentages of oxides. The percentages of sodium oxide decreased by 8.20 %, aluminum oxide by 4.55 %, calcium oxide by 19.82 % and iron oxide by 5.07 % while the percentage of sulfur dioxide increased by 6.27 %, and phosphorus oxide by 7.64 %. The SEM showed the flatness of the surface and the homogeneity of the granules before, and after infected. There were the increased disintegration of the granules, the increased displacement of metal atoms on the surface, cracking, the accumulation of organic and inorganic particulate matter in the cracks, and the spread of saturated fatty acids from Paint and its crystallization on the surface of the paint (Montagner et al., 2013) that caused the formation of metallic soap leading to the deterioration of the colours and the colour medium (Gomart, 2002) (Plate 4 **e, f**). The darkening of the colour was explained as a result of the fact that the anhydrous hematite was converted to iron hydroxide due to humid conditions whereas a partial conversion of the colour to red. Fe_2O_3 turned into black Fe_3O_4 (Maguregui et al., 2014).
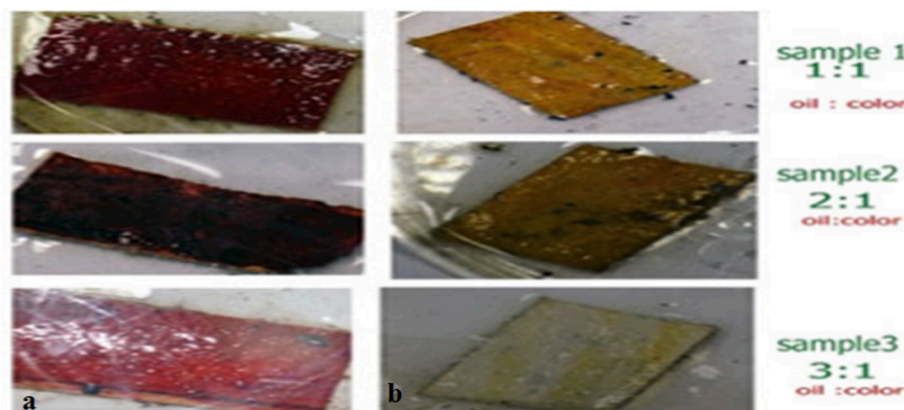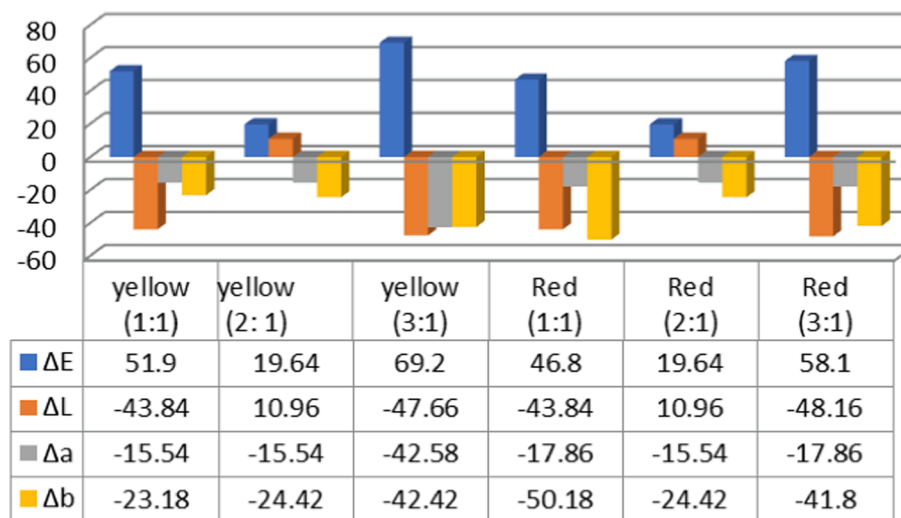
3.3. Examination and analysis by USB digital microscope

The examination using a digital microscope connected to a camera and with a magnification power of 100 X. There was a loss of adhesive force between the colour atoms on the surface (Walsh-Korb & Avérous, 2019). The fungi fed on the minerals involved in the colour, and a vibrant black film and whiteness on the surface of the sample were present (Plate 5).

The ratio of fungal spread after infection was different in both colours. In (1 oil: 1 colour), the ratio was 25 % in red colour with white mycelium and black spores while the ratio was less 25 % with localized spore formation. Furthermore, (2 oil: 1 colour) had different fungal distribution for both colours; definite localized with 50 % spore formation for red colour while 25 % distributed spore location. Finally,

Table 2
Colourimetric measurements before and after fungal infection.

Colour	Before			After		
Colour mixed with oil	b*	a*	L*	b*	a*	L*
Yellow (1colour:1oil)	45.98	12.05	43.25	69.16	29.91	87.09
Yellow (1colour:2oil)	25.75	−1.09	77.23	50.17	14.45	88.19
Yellow (1colour:3oil)	19.61	5.27	17.09	61.41	32.31	65.25
Red(1colour:1 oil)	45.98	12.05	43.25	96.16	29.91	87.09
Red(1colour:2 oil)	25.75	−1.09	87.19	50.17	14.45	76.23
Red(1colour:3 oil)	19.61	5.27	17.09	61.41	23.13	65.25

Table 3
the rate of change (ΔL, Δa, Δb, ΔE) before and after fungal infection for both colours.

	yellow (1:1)	yellow (2:1)	yellow (3:1)	Red (1:1)	Red (2:1)	Red (3:1)
■ ΔE	51.9	19.64	69.2	46.8	19.64	58.1
■ ΔL	-43.84	10.96	-47.66	-43.84	10.96	-48.16
■ Δa	-15.54	-15.54	-42.58	-17.86	-15.54	-17.86
■ Δb	-23.18	-24.42	-42.42	-50.18	-24.42	-41.8

Plate 2. the rate of change (ΔL, Δa, Δb, ΔE) before and after fungal infection for both colours.

according to (3oil: 1 colour), 75 % black and white presentations in red colour besides more than 75 % with distribution of black spores more than white hyphae in yellow colour.

3.4. Raman analysis

The sample of red colour of (1:1) by using a Raman microscope with 20X magnification and a 785 nm laser with a power of 10 microwatts and a time of 10 s was analyzed. The uninfected Red ocher with fungi found in the Raman spectrum at a range of (282, 216——653 – 612) cm^{-1} Feldspar, which is characterized by a Raman spectrum at (356, 653, and 1086) cm^{-1}. It showed the surface regularity and homogeneity of the grains, while the samples infected with fungi that were analyzed and examined with a microscope Raman under the same conditions as before showed the heterogeneity of the grains and their spread fungi on the surface and their penetration into the layer of colours, and dots of green and black were scattered on the surface of the sample around some of the fungal colonies (Fig. 4) as a result of the fungal activities of some strains that reduced iron (II) to iron (III), and the appearance of the same compounds as the previous ones as a result of the fungal activities of some strains that reduced iron (II) to iron III), and the appearance after infected the same compounds as the previous ones. In addition to the appearance of the spectrum of monohydrated and tetrahydrated ferrous sulphate due to the presence of the sulphur ion in the range 158–234-460. Black magnetite presented at 667 cm^{-1} (Bouchard and Smith, 2003) and brown natrojarosite, NaFe$_3$(SO$_4$)$_2$(OH)$_6$ resulted from some microbial activities leading to brown-coloured jarosite in the range of (190,270,375,441,461,574,625,1017,1056,1135,1170) cm^{-1}, siderite in the range of 190–285, and calcium oxalate in the ranges of 530 cm^{-1}, and 574 cm^{-1} (Martens et al., 2003). The curves for iron sulphate and magnetite were not sharp and indicated the formation of weak amorphous compounds that were not cohesive and easily volatile (no solid crystals were formed). While the red colour sample mixed with a ratio of (2 oil: 1 colour) before infection with the fungus showed the presence of hematite (Fe$_2$O$_3$) in the range of (427 cm-1, 449, 467, 495, 527, 549, 559, 590, and 637) cm^{-1} besides the presence of feldspar, by the Raman spectrum with a range at (371, 652, and 1005) cm^{-1}. The surface appeared regular and with homogeneous grains while the fungal-infected samples that were analyzed and examined with a Raman microscope under the same previous conditions showed the same previous results, with an increment in microbial activity with increasing the concentration of linseed oil, in addition to finding magnetite with a wide range at (659) cm^{-1}and jarosite KFe$_3$(SO$_4$)$_2$(OH)$_6$ at a range of (277, 313, 371, 400, 435, 465, 495, 525, 545, 583, 607,645) cm^{-1}. Likewise, the Raman spectra of natrojarosite NaFe$_3$(SO$_4$)$_2$(OH)$_6$ appeared at the range of (435) cm^{-1}, calcium oxalate, magnesium and calcium phosphate were detected on the
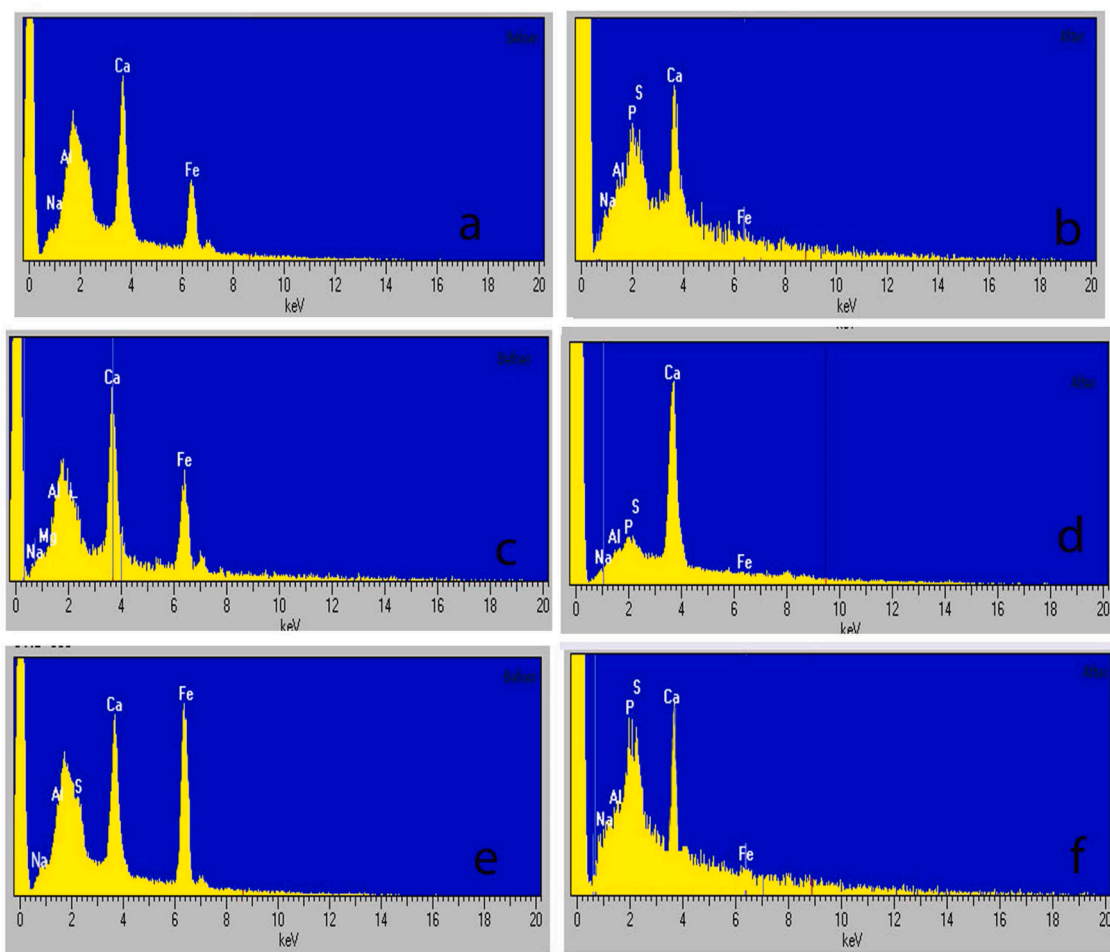
Fig. 2. EDX analysis of red samples (a, c, e); before fungal infection and (b, d, f); after fungal infection.

surface as a result of microbial activity biofilm such as Magnesium oxalate di hydrate at the range of (381—477 – 537—595 –857—918-1736—1460- 1483—1734) cm^{-1},calcium oxalate dihydrate in the range of (918,927,1414, 483,1612) cm^{-1}, calcium phosphate at of (454, 477, 595,952,964,1014,1083) cm^{-1} ferrous sulfate monohydrate at (637—665—1062—1105—1206), ferrous sulfate tetrahydrate at (607—659-1156—988- 1062—1105- 1178) cm^{-1} and ferrous sulfate heptahydrate at (631—964- 1112—1156) cm^{-1}. Raman's analysis of the red parts of samples mixed with linseed oil in a ratio of 3:1 colour oil, not infected with fungi, demonstrated the presence of hematite (Fe$_2$O$_3$) which is characterized by a Raman spectrum at (225, 242, 278, 435, 465, 495, 525, 545, 583, 603, 645, 680) cm^{-1} and feldspar was present in a range at (365, 680, and 1012) cm^{-1}. Surface regularity and homogeneity of the granules occurred while the samples infected with the fungi that were analyzed and examined with a Raman microscope under the same previous conditions showed the spread of the fungi on the surface, their penetration into the layer, and the colour change to black in some parts and Raman analysis of it proved the presence of the same previous compounds, in addition to damage products from compounds such as iron (II) sulfide (FeS) at (277 st, 338) cm^{-1}, the presence of magnetite at (656, 640) cm^{-1} and the presence of calcium and magnesium phosphate besides their oxalates were results of fungal secretions on the surface, so magnesium oxalate di hydrate appeared at a range of (233–379,853,872,854,1014,1110,1481,1644,1757,2889,2944) cm^1 Moreover, calcium oxalate dihydrate at of (534–908-1405–1481) cm^{-1}, calcium phosphate at (264—490- 597—640- 958—1058- 1084) cm^{-1}, ferrous sulfate monohydrate at (640—656- 1110—1211) cm^{-1}, ferrous sulfate tetrahydrate at range (640——1174- 1014—1110) cm^{-1}, ferrous

sulfate heptahydrate at the range (958——1110 – 1151, –1174) cm^{-1} were observed. This occurred due to the influence of fungi and hydrolysis (removal of the ester) produced carboxylic acid groups that may react with dyes to form carboxylic salts (Fig. 4).

Presentation of fungal distribution appeared more obviously with (1 oil: 1 colour) with 80 % fungal spread with all spore formation while (3 oil: 1 colour) had 75 % fungal distribution with majority of spores. Less than 75 % presented in (2 oil: 1 colour) with less white mycelim distribution.

The yellow colour samples examination using a Raman microscope for both infected and uninfected samples. At (1:1) ratio yellow ocher was present at (601, 613, 482, 566, 1085, 1153, 89, 279, 415, 382, 232, 1421, 1297, 154) cm^{-1}, Goethite at (232,279,372,482,589) cm^{-1}and the presence of Feldspar which was characterized at (336, 663 and 1013) cm^{-1}. The Raman microscope showed surface regularity and homogeneity of the grains. As the samples were infected with fungi, it showed surface irregularities and colour changes in some areas and the spread of fungi on the surface. The analysis showed the presence of the same previous compounds in addition to compounds that caused colour changes after microbial infection, such as magnetite at 658, magnesium oxalate dihydrate at (245, 221, 1728, 1624 and 1468) cm^{-1}, calcium oxalate dihydrate at (517, 1486, 1413, 908, 517) cm^{-1}, calcium phosphate at(429——445 – 572——559 – 625——982 – 1039——1061 – 1085) cm^{-1}, ferrous sulfate monohydrate at (613—625- 669—1061 – 1085—1262) cm^{-1}, ferrous sulfate tetrahydrate at (609—658-998—1071- 1093—1141- 1169) cm^{-1}, ferrous sulfate heptahydrate at (1162,976,613,1153) cm^{-1} were found. By comparing the intensity and areas of the absorption spectrum of the functional groups in the samples

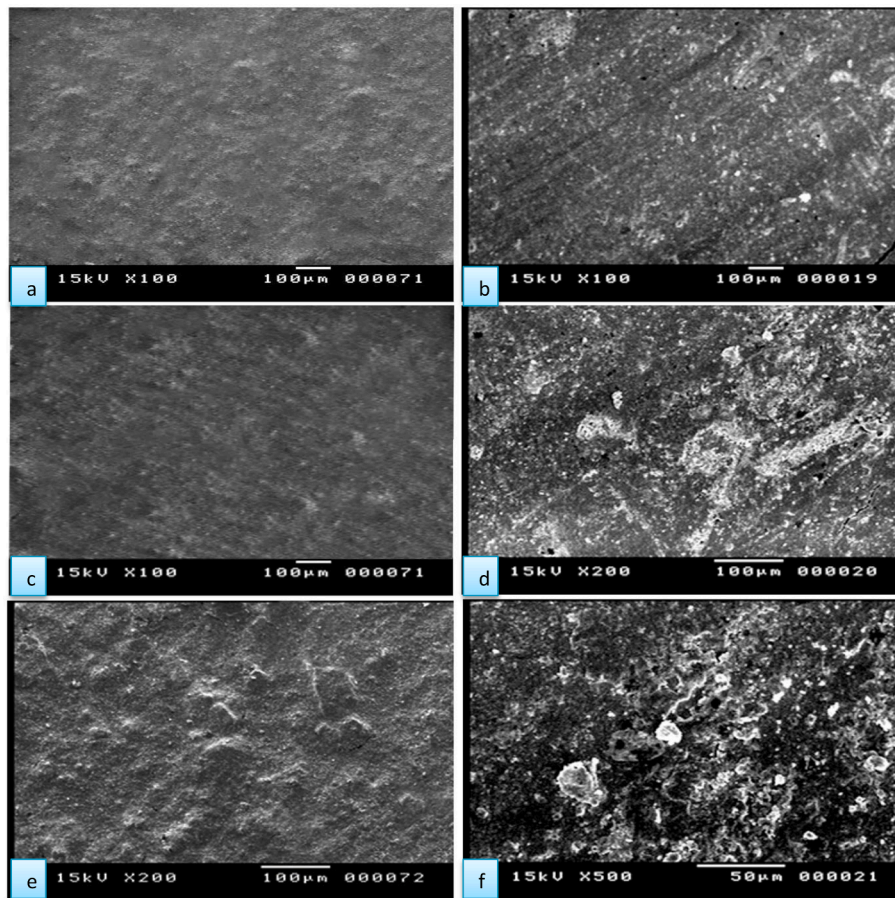**Plate 3.** SEM analysis of red samples (a, c, e); before fungal infection and (b, d, f); after fungal infection.
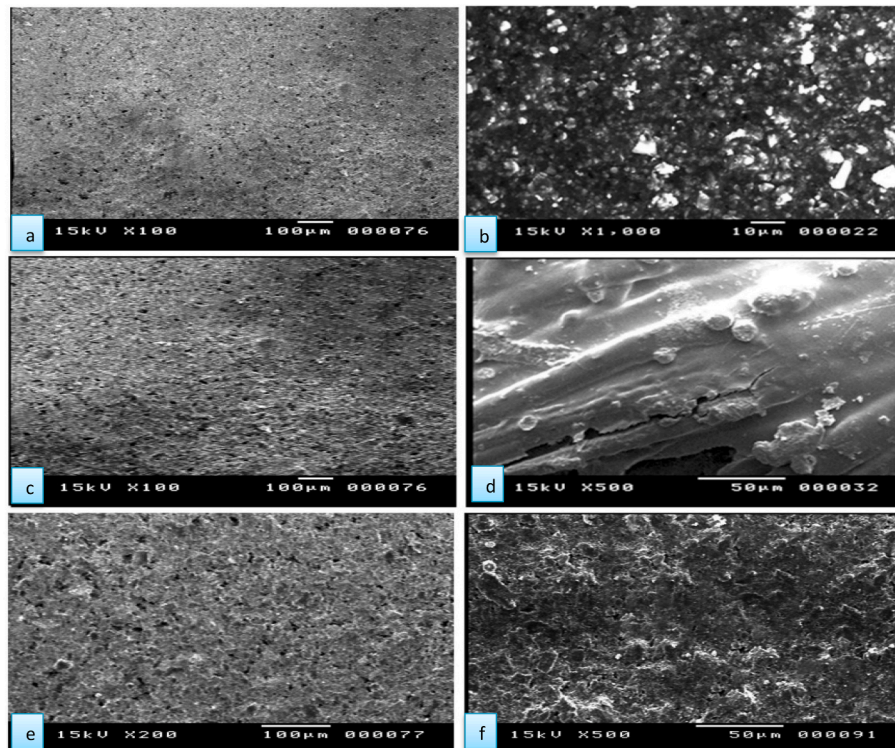

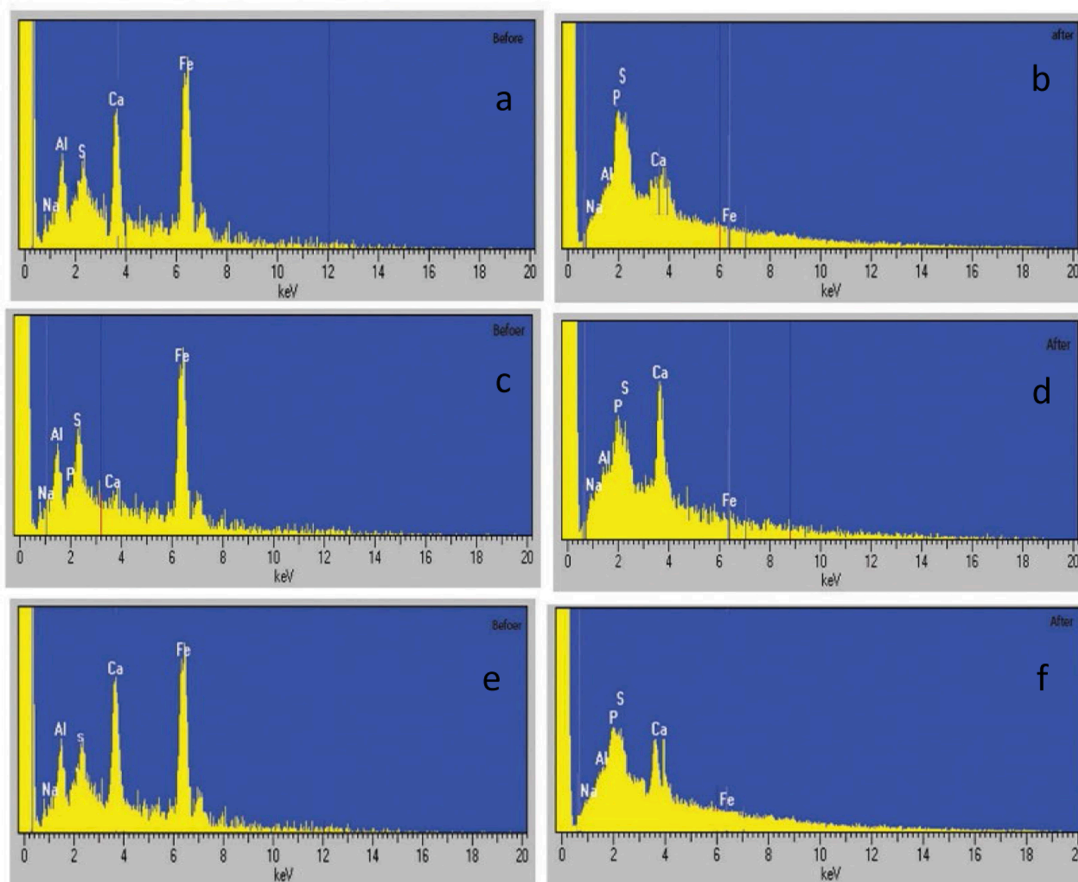**Plate 4.** SEM analysis of red samples (a, c, e); before fungal infection and (b, d, f); after fungal infection.

Fig. 3. EDX analysis of yellow samples (a, c, e); before fungal infection and (b, d, f); after fungal infection.
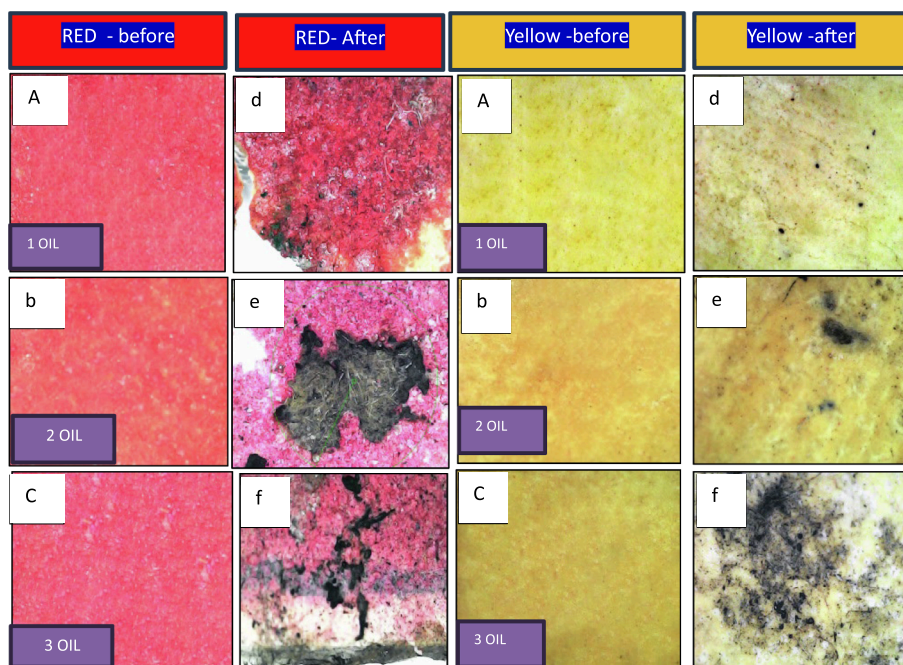

Plate 5. USB analysis of red and yellow samples (1, 2, 3) mixed with linseed oil, (a, b, c); before fungal infection and (d, e, f); after fungal infection.

that were exposed to infection and those that were not infected, it became clear that the intensity increased and the areas of absorption decreased, causing chemical changes and chemical transformations, such as the transformation of iron (III) into iron (II), a colour change into dark yellow, brown (Fig. 5). As the Raman analysis of yellow samples mixed with linseed oil in a ratio of (2 oil: 1 colour) which were not
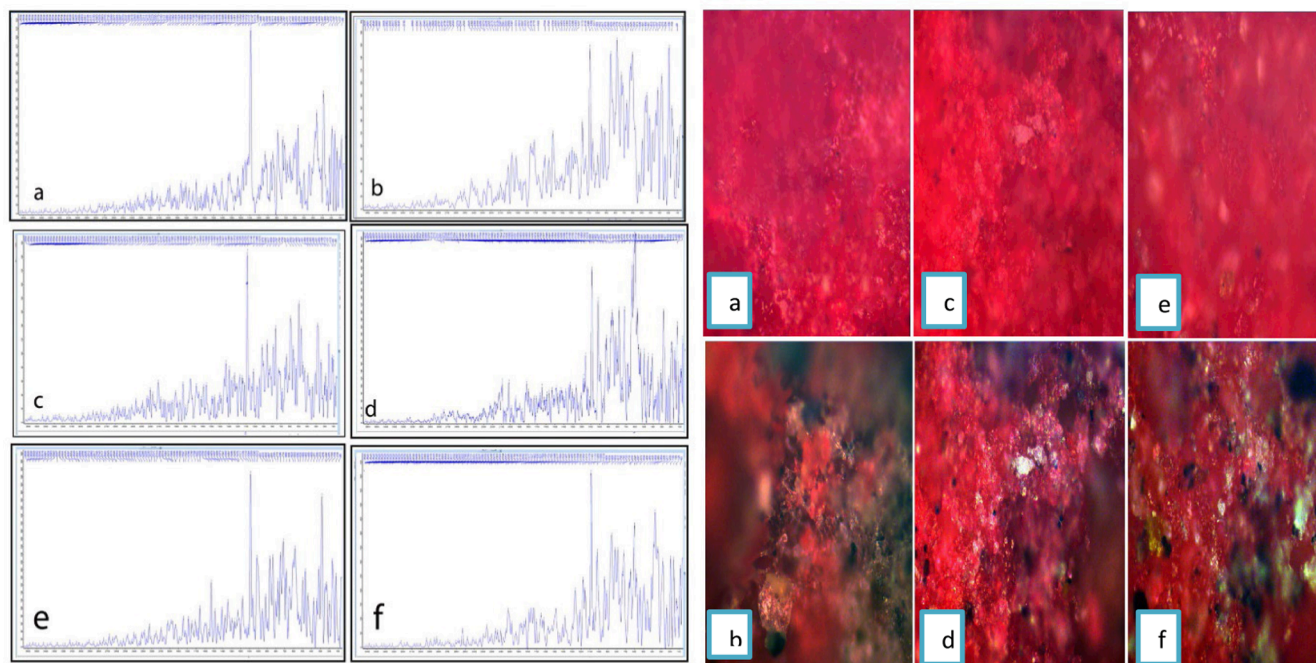
Fig. 4. Red colour samples with Raman spectra (left hand) and with Raman microscope (right hand), A ratio (1:1) (a) before infection, (b) after infection, A ratio of (1:2) (c) before infection and (d) after infection, A ratio (1: 3) (e) before infection, (f) after infection.

Fig. 5. Yellow colour samples with Raman spectra (right hand) and with Raman microscope (left hand), A ratio (1:1) (a) before infection, (b) after infection, A ratio of (1:2) (c) before infection and (d) after infection, A ratio (1: 3) (e) before infection, (f) after infection.
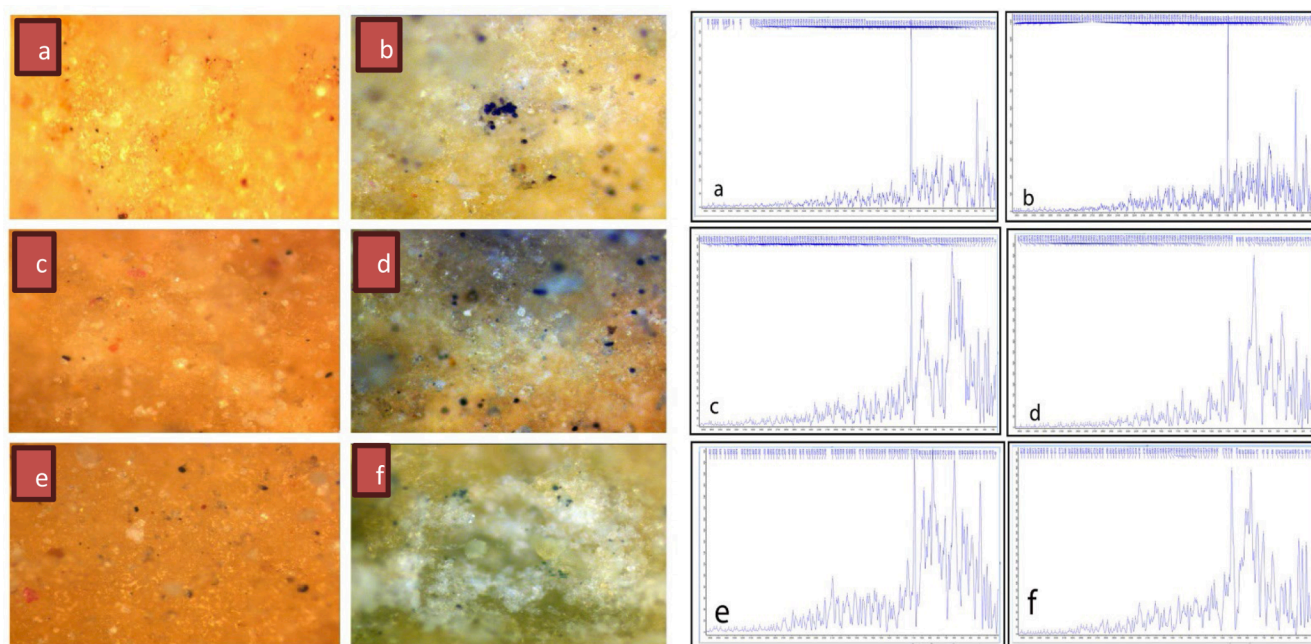
infected with fungi, it was proven that yellow ocher was present at $(153–232-370–415-272–1085-541–493-622—1436-1297)$ cm^{-1}, Goethite at $(1370, 1325, 232, 493, 1599)$ cm^{-1} besides the presence of feldspar which was characterized by the Raman at $(370, 622,$ and $994)$ cm^{-1}. The Raman microscope before the infected showed regularity of the surface and homogeneity of the grains, and it became clear after microbial infection. Homogeneouss of the grains, colour change in some areas, and the spread of fungi on the surface were present (Fig. 5). The analysis showed the presence of the same previous compounds, in

addition to compounds that caused colour changes after microbial infection, such as magnetite at 672, magnesium oxalate dihydrate at $(226—323-451–538-587–847-920–1460-1645–1720)$ cm^{-1}, calcium oxalate dihydrate at $(500–920-1423–1660-1611)$ cm^{-1}, calcium phosphate at $(451–587-611–960 – 1054—1084)$ cm^{-1}, ferrous sulfate monohydrate at $(611—644- 672–1084- 1126)$ cm^{-1}, ferrous sulfate tetrahydrate in the range of $(611—644- 1054–1084- 1162)$ cm^{-1}, ferrous sulfate heptahydrate in the range of $(1162—960- 1100)$ cm^{-1} and sulfur is at $(156–226-483–323)$ cm^{-1}. By comparing the intensity

and areas of the absorption spectrum of the functional groups in the samples that were exposed to infection and those that were not infected, it became clear that the intensity increased, the intensity increased and the areas of absorption decreased, causing chemical changes and chemical transformations to occur, as well as the yellow colour turned to dark yellow and brown due to the transformation of iron (III) into iron (III). The Raman analysis of the yellow parts of samples mixed with linseed oil (3 oil: 1 colour), as (Fig. 5) which were not infected with fungi, demonstrated the presence of Goethite at (279, 441, 498, 597, 636, 665, 711, and 994) cm^{-1} and the presence of feldspar which was characterized in the Raman spectrum at (383, 665, and 994). The Raman microscope showed surface regularity, grain homogeneity, and the clear yellow colour of the sample. However, samples infected with fungi showed surface irregularities, grain heterogeneity, yellow colour change in some areas, the spread of mineral soap on the surface, and fungal secretions of organic acids on the surface (Fig. 5). The analysis showed the presence of the same previous compounds, in addition to compounds that cause colour changes after microbial infection, such as magnetite at (653) cm^{-1}, the presence of magnesium oxalate dihydrate at (237–442-532–569-853–918-1451–1479-1663–1723) cm^{-1}, calcium oxalate dihydrate at (237–442-532–569-853–918-1451–1479-1663–1723) cm^{-1}, calcium phosphate at(442–596-947–1086) cm^{-1}, the presence of ferrous sulfate monohydrate at (616–653-1018–1086-1145) cm^{-1}, the presence of ferrous sulfate tetrahydrate at(1018–1086-114. 5—1172) cm^{-1} and ferrous sulfate heptahydrate at (613 shoulders – 989—1116 – 1145) cm^{-1}. By comparing the intensity and areas of the absorption spectrum of the functional groups in the samples not infected with the fungi and infected, it became clear that the intensity increased after infection and the areas of absorption decreased, causing chemical changes and the yellow colour changing to dark yellow and brown (Fig. 5).

Analyzing the medium in the samples using a Raman microscope with a magnification of group of oil (Table 4) showed the extent of the increase in aliphatic esterification or saponification in the red and yellow colour samples for both linseed oil used as a medium after microbial infection by comparing the intensity and areas of the absorption spectrum of the functional groups in samples mixed with linseed oil (1:1), (2:1), and (1:3) that were not infected with the fungi and those that were infected. It turned out that the intensity increased after infection in all samples, and the absorption areas increased, causing chemical changes in colours and an increment in the intensity of the Raman curve after infection, especially the mixed samples. With a ratio of 2 oil: 1 colour, linseed oil showed the same behavior according to (Table 4) shown below, and the esterification rate increased with the increment in the concentration of the treated oil. Previous results showed that microbial activity increased with the concentration of linseed oil.

With less localization of spore distributed in (1 oil: colour) with less than 25 %. More than 75 % fungal distribution appeared with more spore formation and white hyphae for (2 oil: 1 colour) and (3 oil: 1 colour) respectively.

3.5. Statistical analysis

The correlated data was very high near to whole integer right number. The differences among variable data was very minute whereas Yellow *vs* Red parameters were highest correlated. Red before and after parameters were recorded less value. The Simple Linear Regression (SLR) curves expressed high positive regressed for all variable data (Table 5, Fig. 6).

4. Discussion

Fungi are microorganisms that degrade inorganic, iron-based colours (along with other metal ions) that are essential for microbial metabolism (Martínez-Ruiz et al., 2020; Costa et al., 2020). *Aspergillus* regards as scavengers of scattered minerals, metals and rare earth element resource. (Jones & Bismarck, 2024). Iron oxide minerals are deposited through microbiological activity (Zhou & Fu, 2020). It absorbs heavy elements in inorganic colours which causes a defect in the colour structure, loss of its cohesion, breaking of cross-links, cracking of the colour layer, colour decay, and the appearance of coloured spots that distort the surface because the complex metabolic microbial activity leads to the emergence of a vital black membrane for the production of melanin by fungi (Zeiner et al., 2021) and the production of organic acids, anionic external polymers and amino acids (Mihajlovski et al., 2015). These metabolites are responsible for the digenetic changes of metals and the occurrence of some chemical reactions such as acid decomposition and oxidative corrosion, which leads to the biological corrosion of coloured metal oxides in painted works of art (Sanmartín et al., 2020). The fungi feed on mineral oxides in the appropriate environment of the medium and produce enzymes and metabolically generated organic acids (such as oxalic acid and citric acid) that have chelating properties through which they weaken the metal–oxygen bond, increase the solubility of some metals and form complexes with the metal cations present on the surface matrix.

This is what the study showed using the Raman spectrometer connected to a Raman microscope on colour samples, and the occurrence of a colour change in samples of both red and yellow mixed with different ratios of oil (1:1)(1:2)(3:1) after fungal infection and the appearance of spoilage products. It leaded to colour change, cracking, and weakness. Analysis of the sample showed a red colour after it was exposed to microbial infection. Meanwhile, testing the sample with a Raman microscope we found the appearance of a spectrum of monohydrated and tetrahydrated ferrous sulphate and magnetite Fe_3O_4. An increment in the intensity of the esterification curve may be observed at about 1745 cm^{-1} in the spectrum after infection as a result of the formation of aliphatic esters or saponification to increase microbial activity (Chio et al., 2005). It was noted that the red colour turned yellow and turned brown as a result of the formation of jarosite $KFe_3(SO_4)_2(OH)_6$ and natrojarosite $NaFe_3(SO_4)_2(OH)_6$ resulting from some microbial activities. Upon the same results, the sample of red colour prepared in a ratio of 3:1 red ocher to linseed oil, but the results did not increase in intensity

Table 4
Analyzing the medium in the samples using a Raman before and after fungal infection.

Samples	Raman intensity Before	Raman intensity after	C = O stretching band of ester group of oil before fungal infection	C = O stretching band of ester group of oil after fungal infection
Red1:1	79	110	1757	1786
Red2:1	70	79	1736	1734
Red3:1	62	160	1749	1757
Yellow1:1	55	120	1758	1747
Yellow2:1	85	98	1744	1740
Yellow3:1	60	100	1756	1786

Table 5
Correlation among comparing data for each colour sample (before & after referred to fungal infection).

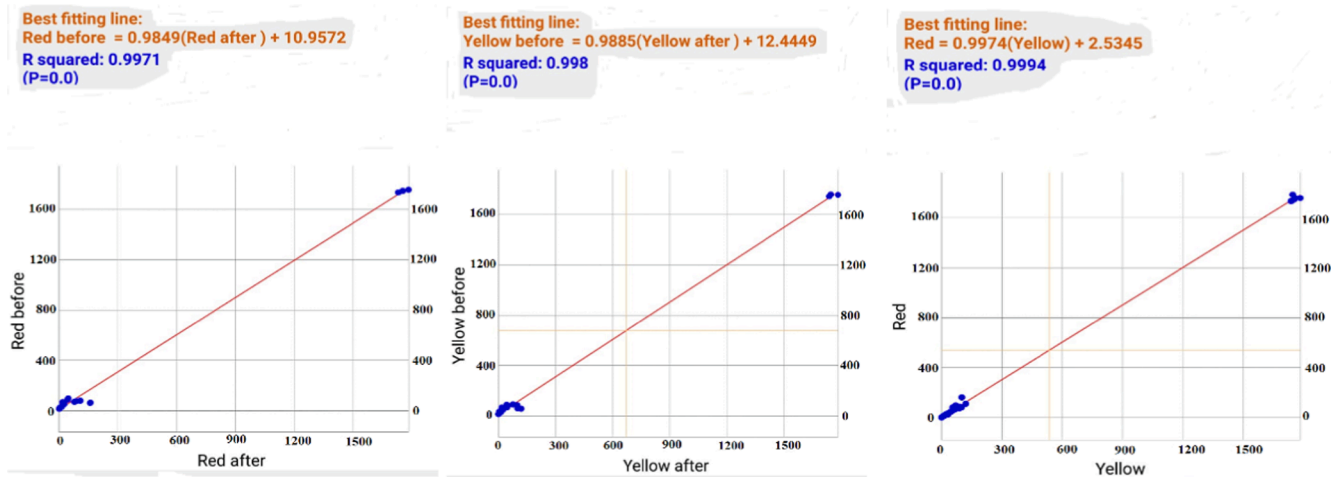|	Red before	Red after	Yellow before	Yellow after	Red	Yellow
Red before	–	0.9986				
Red after	0.9986	–				
Yellow before			–	0.999		
Yellow after			0.999	–		
Red					–	0.9997
Yellow					0.9997	–

Fig. 6. Simple Linear Regression (SLR) curves for each colour sample (before & after referred to fungal infection).

much compared to the sample of red colour No. (3) and the yellow colour analysis appeared after preparing the colour in ratios 1:1 / 1:2. / 1:3. The analysis was carried out under the same testing conditions in the case of the red colour. It was found that more jarosite and natrojarosite were formed and small dots scattered on the colour surface of magnetite on the curve. With an increment in the concentration of linseed oil in the case of doubling and preparing it three times, the colour turned yellow. To a dark brownish colour, and in the event of exposure to fungal infection, scattered shades of blackish green colour were formed as a result of the formation of magnetite and hydrated iron sulphate, in addition to the severe deterioration of linseed oil. The yellow colour at the start of the experiment contained yellow ocher, goethite, and a little jarosite and transformed into jarosite, natrojarosite, magnetite, and iron sulphate after reduction by some fungi. In the case of both red and yellow colours, calcium oxalate, magnesium oxalate, and calcium phosphate were detected on the surface as a result of the microbial activity of the biofilm. SEM-EDX showed the concentration of various mineral elements in the colour layers [red and yellow] before the fungal infection. In both the red and yellow colours, it was noted the presence of sodium oxide, aluminum oxide, calcium oxide, and iron oxide. After the fungal infection, they decreased due to the phenomenon of alkali leaching from the hematite and Goethite particles accompanying them in their composition explained the low proportions because they contain clay containing alkaline and earthy elements of aluminum and silicon. Consequently, aluminum and silicon appeared to have a negative charge on their structure, which can be compensated by cations of alkaline elements such as sodium (Na^+) and calcium (Ca^{2+}), which in turn can be replaced with others ions which gave them the properties of ion exchange. The percentage of alkali were more susceptible to damage and decomposition, and ion exchange resulted in other reactions of cations modifying the alkali, where silicate and alumino silicate minerals were replaced with protons from the free carboxylic acids present in the oily medium, so this process continued. The colour layer was damaged and phosphorus besides sulfur oxide appeared which was likely to be stimulated by fungi. The lack of iron and copper was due to the fact that these organisms needed the heavy metal elements that were present in the composition of the colour itself such as iron. It was considered that living organisms needed most minerals because they provide a number of essential roles including transporting oxygen and the ability to easily switch between ferric (Fe^{2+}) and iron (Fe^{3+}) forms (Kaplan & Kaplan, 2009).

The microscopic examination (USB) showed the abundant growth of fungal hyphae in the form of a black dye, and it spread over all the samples, colour changing and fading. The electron microscopic examination showed the spread of the fungal hyphae on the surface and their entry to the bottom of the layers, so the internal pressure increased and

cracks that were formed over time in the colour layer and the ground, increased (Sayer & Gadd, 2001). Widening of existing cracks leading to mechanical deterioration, "pitting" and the formation of paint blisters (Gadd, 2004) underneath microorganisms which was regarded as a form of biochemical (Adamo & Violante, 2000) weathering separation of the paint layer from the support and fungal chemical activity using nutrients from the colour (Dornieden et al., 2000). Fungal activity produced organic acids that destroy the surface that was more complex than the physical mechanisms taking place through the secretion of various enzymes. Fungal activity catalyzed the decomposition of large molecules into simpler molecules, allowing them to be absorbed and facilitating the penetration of threads into the substrate and the spread of black spots, on the three samples. Such activities leaded to colour decomposition and the occurrence of colour changes. According to colour deterioration, the colour L*a*b* of the red and yellow colour samples infected with fungi mixed with linseed oil in different proportions measured and showed darkness and blackness, and the values of L*a*b* decreased in all samples, which indicated the colour changed and the rate of change of colours differed (Sterflinger & Piñar, 2013; Caneva et al., 2020). Furthermore, the highest rate of change was given by the ΔE values in hematite then goethite mixed with linseed oil in a ratio of (2:1). It was obvious that the presence of dark spots that were due to fungi that died and disappeared from the affected areas and the fungi lead to the formation of secondary minerals such as phosphates, carbonates, sulfides, oxides and oxalates that fungi were able to precipitate phosphate metal from organic materials (López-Miras et al., 2013). On the other hand, the decomposition activities carried out by fungi to maintain growth lead to the separation of the colour layer from the carrier, with the colours being lost and fading due to the secretion of destructive metabolites. The fungi bioleached minerals from muscovite, chromite, malachite, biotite, goethite, galena and hematite deposited them as separated metal species (Kolo & Préat, 2023). From the current study, *Aspergillus* sp. play a role in conserving the environment through bio-weathering and mineral alteration in earth crust as well as they can determine the measure of impurities in crystals and rocks.

5. Conclusion

Many inorganic colours suffer from damage from multiple damage processes from the growth of microorganisms on them. These organisms work on feeding and withdraw the heavy elements that are present within the chemical composition of the coloured materials in the presence of the colour medium as an environment for the living organisms or to feed on them. This is done by through absorption fungi can destroy the colour layer through chemical mechanisms such as the absorption process between heavy metal ions and cellular compounds of biological

types, causing partial decomposition of the coloured materials, loss of colour cohesion, fading and from a physical standpoint, biological pitting, cracking, and peeling. These processes can lead to changes. Aesthetic and structural damage may be irreversible and can permanently impair works of art.

6. Chemical structure list

Aluminum oxide: Al_2O3
Biotite: $K(Mg,Fe)_3AlSi_3O_{10}(OH)_2$
Calcium oxalate: CaC_2O_4
Calcium oxalate dihydrate: $C_2H_4CaO_6$
Calcium phosphate: $Ca_3(PO_4)_2$
Calcium oxide: CaO
Chromite: $FeCr_2O_4$
Feldspar: $KAlSi_3O_8$
Ferrous sulphate heptahydrate: $FeSO_4 \cdot 7H_2O$
Ferrous sulphate monohydrate: $FeSO_4 \cdot H_2O$
Ferrous sulphate tetrahydrate: $FeSO_4 \cdot 4H_2O$
Galena: PbS
Goethite: $\alpha\text{-}Fe^{3+}O(OH)$
Hematite: Fe_2O_3
Iron hydroxide: $Fe(OH)_3$
Iron oxide: FeO
Iron (II) sulfide: FeS
Jarosite $KFe_3(SO_4)_2(OH)_6$
Magnetite: Fe_3O_4
Magnesium oxalate: MgC_2O_4
Magnesium oxalate dihydrate: $C_2H_4MgO_6$
Magnesium phosphate: $Mg_3(PO_4)_2$
Malachite: $CH_6Cu_2O_5$
Muscovite: $KAl_2(AlSi_3O_{10})(F,OH)_2$
Natrojarosite: $NaFe_3(SO_4)_2(OH)_6$
Phosphorus oxide: P_2O_3
Sodium oxide: Na_2O
Sulphur dioxide: SO_2

CRediT authorship contribution statement

Abatable Thanaa: Resources, Methodology. **Mari Sumayli:** Supervision, Software, Investigation, Funding acquisition, Formal analysis. **A. El-Shabasy:** Writing – review & editing, Writing – original draft, Visualization.

Acknowledgment

References

Abada, E., Mashraqi, A., Modafer, Y., Al, M.A., Abboud, A.-S., 2024. Review green synthesis of silver nanoparticles by using plant extracts and their antimicrobial activity. Saudi J. Biol. Sci. 31 (1), 103877.

Adamo, P., Violante, P., 2000. Weathering of rocks and neogenesis of minerals associated with lichen activity. Appl. Clay Sci. 16 (5–6), 229–256.

Armstrong-Totten, J., 2014. A Decade of Change and Compromise: John Smith (1781–1855) and the Selling of Old Master Paintings in the 1830s. British Models of Art Collecting and the American Response 87–100.

Bacci, M., Baldini, F., Carlà, R., Linari, R., 1991. A colour analysis of the Brancacci Chapel frescoes. Appl. Spectrosc. 45 (1), 26–31.

Berg, K.J.V.D., Boon, J.J., Pastorova, I., Spetter, L.F., 2000. Mass spectrometric methodology for the analysis of highly oxidized diterpenoid acids in Old Master paintings. J. Mass Spectrom. 35 (4), 512–533.

Bouchard, M., Smith, D.C., 2003. Catalogue of 45 reference Raman spectra of minerals concerning research in art history or archaeology, especially on corroded metals and coloured glass. Spectrochim. Acta A Mol. Biomol. Spectrosc. 59 (10), 2247–2266.

Bruyn, J., Haak, B., Levie, S.H., Van Thiel, P.J., 2012. A Corpus of Rembrandt Paintings Vol. 1, 1625–1631.

Caneva, G., De Nuntiis, P., Fornaciari, M., Ruga, L., Valenti, P., Pasquariello, G., 2020. Aerobiology applied to the preventive conservation of cultural heritage. Aerobiologia 36, 99–103.

Cañveras, S., Sanchez-Moral, V., Sloer, C., Saiz-Jimenez, J., 2001. Microorganisms and microbially induced fabrics in cave walls. Geomicrobiol J. 18 (3), 223–240.

Carvalho, H.P., Sequeira, S.O., Pinho, D., Trovão, J., da Costa, R.M.F., Egas, C., Portugal, A., 2019. Combining an innovative non-invasive sampling method and high-throughput sequencing to characterize fungal communities on a canvas painting. Int. Biodeter. Biodegr. 145, 104816.

Chio, C.H., Sharma, S.K., Muenow, D.W., 2005. Micro-Raman studies of hydrous ferrous sulfates and jarosites. Spectrochim. Acta A Mol. Biomol. Spectrosc. 61 (10), 2428–2433.

Costa, O.Y., Oguejiofor, C., Zühlke, D., Barreto, C.C., Riedel, K., Kuramae, E.E., 2020. Impact of different trace elements on the growth and proteome of two strains of Granulicella, class "Acidobacteriia". Front. Microbiol. 11, 538660.

Cucci, C., Delaney, J.K., Picollo, M., 2016. Reflectance hyperspectral imaging for investigation of works of art: old master paintings and illuminated manuscripts. Acc. Chem. Res. 49 (10), 2070–2079.

De Viguerie, L., Ducouret, G., Lequeux, F., Moutard-Martin, T., Walter, P., 2009. Historical evolution of oil painting media: A rheological study. C. R. Phys. 10 (7), 612–621.

Dornieden, T., Gorbushina, A.A., Krumbein, W.E., 2000. Biodecay of cultural heritage as a space/time-related ecological situation—an evaluation of a series of studies. Int. Biodeter. Biodegr. 46 (4), 261–270.

Frost, R.L., Weier, M.L., 2003. Raman spectroscopy of natural oxalates at 298 and 77 K. J. Raman Spectrosc. 34 (10), 776–785.

Gadd, G.M., 2004. Mycotransformation of organic and inorganic substrates. Mycologist 18 (2), 60–70.

Gargano, M., Bonizzoni, L., Grifoni, E., Melada, J., Guglielmi, V., Bruni, S., Ludwig, N., 2020. Multi-analytical investigation of panel, pigments and varnish of The Martyirdom of St. Catherine by Gaudenzio Ferrari (16th century). J. Cult. Herit. 46, 289–297.

Gomart, E., 2002. Methadone: Six effects in search of a substance. Soc. Stud. Sci. 32 (1), 93–135.

Grbić, M.L., Stupar, M., Savković, Ž., Jelikić, A., Stanojević, D., Vukojević, J., 2016. Fungal-induced deterioration of mural paintings: In situ and mock-model microscopy analyses. Microsc. Microanal. 22 (2), 410–421.

Jones, M.P., Bismarck, A., 2024. Mycomining: perspective on fungi as scavengers of scattered metal, mineral, and rare earth element resources. RSC Sustainability 2024, 1–6.

Kaplan, C.D., Kaplan, J., 2009. Iron acquisition and transcriptional regulation. Chem. Rev. 109 (10), 4536–4552.

Kolo, K., Préat, A., 2023. In Vitro Experimental Observations on Fungal Colonization, Metalophagus Behavior, Tunneling, Bioleaching and Bioweathering of Multiple Mineral Substrates. Minerals 13, 1540.

Kosman, D.J., 2003. Molecular mechanisms of iron uptake in fungi. Mol. Microbiol. 47 (5), 1185–1197.

Lepot, L., Denoël, S., Gilbert, B., 2006. The technique of the mural paintings of the Tournai Cathedral. J. Raman Spectroscopy 37 (10), 1098–1103.

López-Miras, M., Piñar, G., Romero-Noguera, J., Bolivar-Galiano, F.C., Ettenauer, J., Sterflinger, K., Martin-Sanchez, I., 2013. Microbial communities adhering to the obverse and reverse sides of an oil painting on canvas: identification and evaluation of their biodegradative potential. Aerobiologia 29, 301–314.

Maguregui, M., Castro, K., Morillas, H., Trebolazabala, J., Knuutinen, U., Wiesinger, R., Madariaga, J.M., 2014. Multianalytical approach to explain the darkening process of hematite pigment in paintings from ancient Pompeii after accelerated weathering experiments. Anal. Methods 6 (2), 372–378.

Martens, W., Frost, R.L., Kloprogge, J.T., 2003. Raman spectroscopy of synthetic erythrite, partially dehydrated erythrite and hydrothermally synthesized dehydrated erythrite. J. Raman Spectrosc. 34 (1), 90–95.

Martínez-Ruiz, E.B., Cooper, M., Fastner, J., Szewzyk, U., 2020. Manganese-oxidizing bacteria isolated from natural and technical systems remove cylindrospermopsin. Chemosphere 238, 24625.

Matteini M., Mazzeo R. (2009). Structure of panel and canvas paintings. In *Scientific examination for the investigation of paintings*. A handbook for conservator-restorers, pp. 11-20, Centro Di.

Mihajlovski, A., Seyer, D., Benamara, H., Bousta, F., Di Martino, P., 2015. An overview of techniques for the characterization and quantification of microbial colonization on stone monuments. Ann. Microbiol. 65, 1243–1255.

Monaco, A.L., Marabelli, M., Pelosi, C., Picchio, R., 2011. Colour measurements of surfaces to evaluate the restoration materials. In: O3A: Optics for Arts, Architecture, and Archaeology III, Vol. 8084. SPIE, pp. 189–202.

Montagner, C., Sanches, D., Pedroso, J., Melo, M.J., Vilarigues, M., 2013. Ochres and earths: Matrix and chromophores characterization of 19th and 20th century artist materials. Spectrochim. Acta A Mol. Biomol. Spectrosc. 103, 409–416.

Onofri, S., 2009. Old master paintings, export veto and price formation: An empirical study. Eur. J. Law Econ. 28 (2), 149–161.

Pellerito, C., Di Marco, A.E., Di Natale, M.C., Pignataro, B., Scopelliti, M., Sebastianelli, M., 2016. Scientific studies for the restoration of a wood painting of the Galleria Interdisciplinare Regionale della Sicilia—Palazzo Mirto di Palermo. Microchem. J. 124, 682–692.

Poyatos, F., Morales, F., Nicholson, A.W., Giordano, A., 2018. Physiology of biodeterioration on canvas paintings. J. Cell. Physiol. 233 (4), 2741–2751.

Ranalli, G., Zanardini, E., Sorlini, C., 2009. Biodeterioration–including cultural heritage. In Encyclopedia of microbiology,191–205.

Salvador, C., Bordalo, R., Silva, M., Rosado, T., Candeias, A., Caldeira, A.T., 2017. On the conservation of easel paintings: evaluation of microbial contamination and artists materials. Appl. Phys. A 123, 1–13.

Sanmartín, P., Sanjurjo-Sánchez, J., Prieto, B., 2020. Covering layers on granite buildings of northwestern Iberian Peninsula: When observable characteristics and lab characterization do not match. Coatings 10 (2), 137.

Savković, Ž., Stupar, M., Unković, N., Ivanović, Ž., Blagojević, J., Vukojević, J., Ljaljević Grbić, M., 2019. In vitro biodegradation potential of airborne Aspergilli and Penicillia. The Science of Nature 106, 1–10.

Sayer, J.A., Gadd, G.M., 2001. Binding of cobalt and zinc by organic acids and culture filtrates of Aspergillus niger grown in the absence or presence of insoluble cobalt or zinc phosphate. Mycol. Res. 105 (10), 1261–1267.

Seves, A.M., Sora, S., Scicolone, G., Testa, G., Bonfatti, A.M., Rossi, E., Seves, A., 2000. Effect of thermal accelerated ageing on the properties of model canvas paintings. J. Cult. Herit. 1 (3), 315–322.

Sterflinger, K., Piñar, G., 2013. Microbial deterioration of cultural heritage and works of art—tilting at windmills? Appl. Microbiol. Biotechnol. 97, 9637–9646.

Videla, H.A., Guiamet, P.S., de Saravia, S.G., 2000. Biodeterioration of Mayan archaeological sites in the Yucatan Peninsula, Mexico. Int. Biodeterior. Biodegrad. 46 (4), 335–341.

Walsh-Korb, Z., Avérous, L., 2019. Recent developments in the conservation of materials properties of historical wood. Prog. Mater Sci. 102, 167–221.

Zeiner, C.A., Purvine, S.O., Zink, E., Paša-Tolić, L., Chaput, D.L., Santelli, C.M., Hansel, C.M., 2021. Mechanisms of manganese (II) oxidation by filamentous ascomycete fungi vary with species and time as a function of secretome composition. Front. Microbiol. 12, 610497.

Zhou, H., Fu, C., 2020. Manganese-oxidizing microbes and biogenic manganese oxides: characterization, Mn (II) oxidation mechanism and environmental relevance. Rev. Environ. Sci. BioTechnol. 19 (3), 489–507.